Infrared absorption by laterally modulated two-dimensional electron systems

W. L. Schaich, P. W. Park,* and A. H. MacDonald
Department of Physics, Indiana University, Bloomington, Indiana 47405
(Received 11 March 1992)

We present model calculations of far-infrared absorption by the combined system of a grating coupler plus a laterally modulated two-dimensional electron gas. The response of the electron gas to the optical fields has been determined in a companion paper and the grating is described as a planar sheet with alternating strips of different conductivity. By varying parameters for the strength and period of the modulation the fractional change of transmission through the system is examined in different response regimes. We find that a single peak can dominate the spectra in certain limits although the physical origin of this peak varies. It can arise from a single intersubband transition or be due to either running or confined plasmon modes. In the crossover regions between these limits there is no simple behavior in the spectra.

I. INTRODUCTION

In the preceding paper,[1] referred to here as I, we presented model calculations of the density-response functions χ^0 and χ of laterally structured two-dimensional electron systems (LS2DEG). We now use these results as input for evaluations of the infrared absorption by such systems when they are combined with a nearby planar grating. This scheme for enhancing the coupling of radiation to electronic excitations is fairly common,[2,3] but a theory that allows for spatial modulation in both the LS2DEG and the grating has not been presented before, to our knowledge. Our analysis of the fractional change in transmission, $\Delta T/T$, between the presence and absence of the LS2DEG is summarized in Sec. II. This theory is a straightforward, but algebraically involved, extension of an earlier treatment that ignored nonlocality and inhomogeneity in the electronic response.[4] A detailed list of the required matching equations is given in the Appendix. In Sec. III we illustrate the theory with parameter choices for the LS2DEG identical to those used in I. We thus have the same physical system but now examine its response through the filter of an infrared transmission experiment. This approach is useful in allowing one to see which response characteristics are revealed and which are missed by this experimental probe.

II. BASIC EQUATIONS

The configuration of the grating coupler and the LS2DEG has the two planar systems parallel to each other and separated by much less than the (propagating) wavelength of the infrared radiation, which moves along the common normal that defines the x direction. The background dielectric in which the LS2DEG is embedded and on which the grating sits is described by the dielectric constants

$$\epsilon(x)=\begin{cases}1, & x<0\\ \epsilon_0, & 0<x<h\\ \epsilon_s, & h<x\ ,\end{cases} \tag{1}$$

where in our calculations h will be less than 50 nm and $\epsilon_0=\epsilon_s=\epsilon$. We evaluate the probability for the incident radiation, coming from vacuum in $x<0$, to propagate into the bulk substrate where $x>h$.

Both the grating and the LS2DEG are assumed to have negligible thickness and to be corrugated in a single, common direction which defines the y axis. There is no variation in the plane along the z direction. The modulation in the LS2DEG is represented by a Kronig-Penney (KP) model, as described in I. For the grating the corrugation is characterized by the (two-dimensional, local) resistivity profile

$$\rho(y)=\begin{cases}\rho_h, & |y|<a/2\\ \rho_l, & a/2<|y|<d/2\ ,\end{cases} \tag{2}$$

plus its periodic extension into $|y|>d/2$. The high-resistivity strips are centered over the wells of the KP model. We acknowledge that our simple description of the grating is not a perfect fit to any one of the various experimental constructions,[2,3,5–9] but it is theoretically quite tractable. For more realistic grating shapes one needs more involved grating theories,[10] even if one just allows for finite thickness.[11] However, we do not expect that new qualitative influences of the grating coupler on infrared transmission spectra would result from more structured models. The only obvious exception to this claim comes from broken symmetry. Our models of both the grating and the LS2DEG have imposed inversion symmetry within the y-z plane, which in turn leads to parity-based selection rules for excitation strengths. Removing this symmetry will affect the number of peaks that appear in $\Delta T/T$. Specific cases where this should occur will be noted in Sec. III.

We next consider how a model system defined by Eqs. (1) and (2) and a KP modulation potential responds to infrared radiation. The microscopic matching equations are listed in the Appendix. Here we summarize only the essential ingredients. Compared to the earlier analysis,[4] we have the simplifications of no static magnetic field and sufficient symmetry that the responses to y- and z-polarized light can be treated separately. For the latter case, where the electric vector points along the grating

strips, the grating efficiently shields the LS2DEG from the incident beam, if $\rho_l \ll 4\pi/c = 377\ \Omega$. Thus only the orthogonal polarization is of physical interest and we will examine it alone, at the same time omitting Cartesian subscripts from vectors, tensors, etc. since all components will be in the y direction.

The transmission coefficient is then

$$T = \sqrt{\epsilon_s}\,|t|^2 , \tag{3}$$

where the transmission amplitude is

$$t = \frac{2}{1+\sqrt{\epsilon_s}+\frac{4\pi}{c}\Sigma} \tag{4}$$

with Σ the y,y element of the macroscopic surface conductance. We compute Σ by adding together the spatially averaged currents in the grating and the LS2DEG and dividing by e, the average strength of the electric field near the surface,

$$\Sigma = j_0/e + \left[\sigma(0,0) + \sum_{n>0} \sigma(0,n) t_n / e\right] . \tag{5}$$

The averaged current in the grating is j_0 while that in the LS2DEG has been expressed in terms of the (two-dimensional) conductivity elements $\sigma(n,m)$. Their unit is Ω^{-1} and they require two wave-vector arguments since the response is both nonlocal and inhomogeneous. Our assumption of inversion symmetry within the y-z plane allows us to work with cosine Fourier transforms so that

$$\sigma(n,m) = \left[\frac{2-\delta_{n,0}}{d}\right] \int_{-d/2}^{d/2} dy \int_{-\infty}^{\infty} dy' \cos(G_n y)\sigma(y,y')\cos(G_m y') , \tag{6}$$

with $G_n = n(2\pi/d)$. The remaining factor t_n in Eq. (5) is also a cosine Fourier transform: that at wave vector G_n of the fluctuating electric field along $\hat{y}$ in the plane of the LS2DEG.

To calculate j_0 and the t_n requires the microscopic analysis outlined in the Appendix. This is developed in terms of the $\sigma(n,m)$ of the LS2DEG and the

$$\rho_n = \left[\frac{2-\delta_{n,0}}{d}\right] \int_{-d/2}^{d/2} dy \cos(G_n y)\rho(y) \tag{7}$$

of the grating. The $\sigma(n,m)$ are related to the (double) Fourier transform coefficients $\sigma_{n,m}$ by

$$\sigma(n,m) = (1-\tfrac{1}{2}\delta_{n,0})[\sigma_{n,m}+\sigma_{n,-m}] \tag{8}$$

and the $\sigma_{n,m}$ are in turn related through the equation of continuity to the density-response functions that were calculated in I:

$$\sigma_{n,m} = \frac{i\omega e^2}{G_n G_m}\chi^0_{n,m}(q\to 0,\omega) , \tag{9}$$

where ω is the driving frequency. The form of Eqs. (8) and (9) shows that there is less information in the $\sigma(n,m)$ than in the $\chi^0_{n,m}$ and is the algebraic way that parity-based constraints enter the grating theory. The key matrix that describes the effect of Coulomb interactions is $D^{-1}(n,m)$, where

$$D(n,m) = [\epsilon_s + \epsilon_0 \coth(G_n h)]\delta_{n,m} + \frac{4\pi i n}{\nu d c}\sigma(n,m) , \tag{10}$$

with $2\pi c\nu = \omega$. Our calculations will show that the influence of the grating on collective-mode locations is well described by replacing the (uniform) background dielectric constant ϵ with an effective dielectric constant $\frac{1}{2}[\epsilon_s + \epsilon_0 \coth(G_n h)]$

III. MODEL CALCULATIONS

We consider results for LS2DEG in each of the four distinct response regimes described in I (see Fig. I 1) and plot the fractional change in transmission through the system as a function of the infrared frequency, scaled by the energy unit $t = \hbar^2\pi^2/2m^* d^2$. The primary inputs for the calculations are the $\chi^0_{n,m}$, whose diagonal imaginary parts are plotted in I, plus the high- and low-resistivity values in the grating, for which we use $\rho_h = 1000\ \Omega$ and $\rho_l = 2\ \Omega$. The maximum wave vector for which the $\sigma(n,m)$ are nonzero is the same as used for the $\chi^0_{n,m}$ in I while the cutoff for the ρ_n of Eq. (7) is double this value. The height h of the grating above the LS2DEG is chosen to be much smaller than, but roughly scaling with, the modulation period d. Since in our model experimental configuration the infrared absorption at different accessible wave vectors cannot be separately measured, we will have only one plot of $\Delta T/T$ in each case to compare with the several panels of peaks for the imaginary parts of the $\chi_{n,n}$ shown in I.

We begin with a LS2DEG in the long period, weak modulation limit. Its KP parameters are period $d = 450$ nm, well width $a = 300$ nm, and barrier height $V/t = 50$. Results for $\Delta T/T$ when $h = 40$ nm are shown in Fig. 1, which should be compared to Fig. I 4, with the caution that the vertical scale in I is relative while that for $\Delta T/T$ is absolute. The rise that grows off scale as $\omega \to 0$ in Fig. 1 is from Drude absorption in the LS2DEG. It appears mathematically in $\sigma(0,0)$, which describes the averaged current in the LS2DEG driven by the averaged field. The fine structure on the Drude tail is due to some of the single-particle peaks evident in the χ^0 plots of Fig. I 4. It is not obvious though which specific low-frequency peaks in Fig. I 4 appear (shifted in location and strength) in Fig. 1. For the plasmon peaks, starting at $\hbar\omega/t = 132.5$, it is easier to identify the physical origins, although only the first peak is strong. The $n = 1,2,3,4$ peaks corresponding to the four panels shown in Fig. I 4 appear slightly red-shifted in Fig. 1 near $\hbar\omega/t = 132.5, 228.5, 302.0, 359.5$, respectively. The strength of these plasmon peaks depends on the efficiency of excitation of the different umklapp channels, which in general requires our full self-consistent calculation to determine. It is however possi-

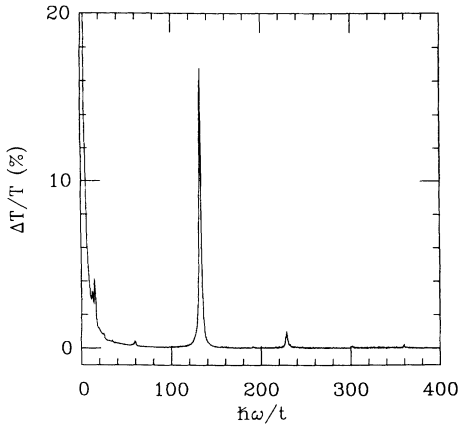

FIG. 1. Fractional change in transmission $\Delta T/T$ vs photon energy $\hbar\omega$. The energy unit is $t=0.028$ meV. The LS2DEG and grating parameters are given in the text. The dominant excitation is a running plasmon wave.

ble to discern certain qualitative aspects in special limits.

For Fig. 1 the appropriate limits to consider are those of a uniform 2D electron gas[12] and a perturbative influence of the grating.[4] Then the coupling to nonzero G_n in the electron gas depends on the grating alone and involves factors of ρ_n^2 and $e^{-2G_n h}$. The latter shows why we have chosen $h \ll d$ and (partially) explains why the peaks due to excitations at larger G_n are systematically suppressed in $\Delta T/T$. Reducing h can enhance their strength, but they also can be modified via the ρ_n, which in our simple grating model are given by

$$\rho_{n\neq 0}=\frac{2}{\pi n}(\rho_h-\rho_l)\sin\left[\frac{n\pi a}{d}\right] . \tag{11}$$

For the case of Fig. 1 (and Fig. 2 below), where $a/d=\frac{2}{3}$, one has $\rho_3=0$, which (almost) eliminates the $n=3$ peak from plots such as Fig. 1 for any value of h. We emphasize the parenthetical cautions in the above remarks,

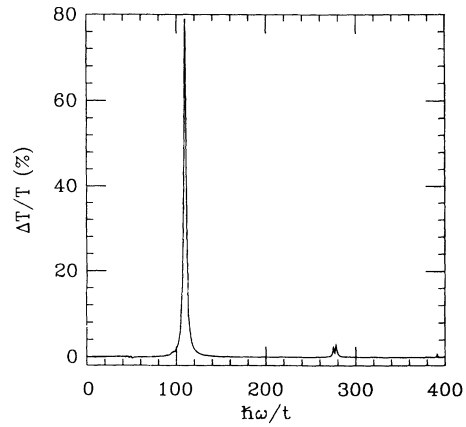

FIG. 2. Fractional change in transmission $\Delta T/T$ vs photon energy $\hbar\omega$. All parameter values are the same as for Fig. 1, except the KP barrier height which has been increased to $V/t=500$. The dominant excitation is a confined plasmon.

which are necessary since the LS2DEG is not strictly uniform here and since the perturbation theory of the grating is not sufficient when peaks in $\Delta T/T$ become strong and sharp.[4]

Similar cautions are necessary when one tries to understand peak positions based on the diagonal element of the D matrix in Eq. (10), since there is no reference there to the resistivity of the grating. Still, for our choice of ρ_h, associating a peak with the frequency at which the real part of these elements vanish provides a simple and remarkably accurate estimate for the slight shift in peak positions between Figs. I 4 and 1. If we suppress the resistivity modulation in the grating by setting $\rho_l=\rho_h=1000\ \Omega$, the plasmon peak positions in Fig. 1 are unchanged to within $0.5t$. The peak heights are, however, considerably reduced since most of the source of umklapp scattering has been removed. The $n=1$ peak, for instance, drops to a height of $\Delta T/T=0.4\%$. We can also remove the shift of peak locations between Figs. I 4 and 1 if we completely suppress the grating influence by going to the limit of an isolated LS2DEG. This requires a slight reformulation of the basic equations since the transmission of interest is then through a LS2DEG immersed in an infinite uniform dielectric. The formal changes are listed in the Appendix. The resulting spectrum is similar to that of Fig. 1 but the peak locations now agree with those in Fig. I 4. The peak strengths are weaker than in Fig. 1, e.g., the $n=1$ peak has $\Delta T/T=1.9\%$.

A further feature can also be addressed with this last calculation. It is clear (at least for $n=1,2$) that our $\Delta T/T$ is sensitive to only one member of the pair of split-plasmon peaks in Fig. I 4. This selectivity arises from the in-plane inversion symmetry that we impose on our model of the LS2DEG and grating. Comparing peak positions between Fig. I 4 and $\Delta T/T$ for an isolated LS2DEG, we find that for $n=1$ the lower-frequency peak is seen, while for $n=2$ the higher-frequency peak survives. Such behavior is easy to understand within the picture of (nearly free) plasmon bands.[13,14] The plasmon properties (e.g., induced charge or field) have definite but opposite parities at a Bragg plane on different sides of a gap. Since the incident field and grating coupler do not break the inversion symmetry, $\Delta T/T$ is only sensitive to modes at either the upper or the lower plasmon band edge. Which member of the pair is seen depends on the sign of the coupling of the two degenerate free plasmons. For the gap at G_n this sign, which we call s_n, is set by that of the cosine Fourier transform of the equilibrium density profile at $2G_n$.[13,14] In the weak modulation limit transforms of the equilibrium density are proportional to transforms of the perturbing potential, which for the LS2DEG has the KP form. These arguments suggest that s_n is determined by $\sin(2\pi n a/d)$, which does change sign between $n=1$ and $n=2$ for $a/d=\frac{2}{3}$. If one removed the inversion symmetry in the grating, we would be able to couple to both members of each split-plasmon pair. This is readily accomplished experimentally by evaporating the metal overlayer from varying angles and one does see (asymmetric) pairs of peaks.[15]

Next we increase the modulation amplitude in the

LS2DEG to move into the regime of confined plasmons. This is accomplished by increasing V/t to 500, while holding all other parameters fixed. Results for $\Delta T/T$ are shown in Fig. 2, which should be compared to Fig. I 7. The lowest confined plasmon produces a very strong peak while the next one, which should be near $220t$, is absent. This selection rule is again a consequence of inversion symmetry, which allows the confined modes to possess a definite symmetry. The structures near $280t$ and $390t$ are less easy to interpret since from Fig. I 7 sharp plasmons do not exist in this energy range; i.e., one has moved out of the confined plasmon limit.

With a strong modulation in the LS2DEG we expect the grating to be of less importance for excitation strengths. To demonstrate this we first set $\rho_l = \rho_h$, which does not move peak locations but does decrease the height of the main peak to $\Delta T/T = 41\%$. Then we go to the isolated LS2DEG limit, which shifts the main peak in $\Delta T/T$ up to $128.0t$ (as in Fig. I 7) and increases its height to 81%. Thus most of the umklapp scattering is being provided by the LS2DEG itself.

In Fig. 3 we plot $\Delta T/T$ for a short period, weak modulation system. Its KP parameters are $d = 50$ nm, $a = 20$ nm, and $V/t = 4$. We also moved the grating closer by setting $h = 5$ nm. There is little to analyze since no strong, sharp peaks appear in Fig. 3, as is expected from Fig. I 9. The Landau damping (due to the short period) is too strong to allow plasmons and the single-particle bands are too broad (due to the weak modulation) to allow dominant intersubband transitions. The rise off scale as $\omega \to 0$ is again due to Drude absorption.

The situation simplifies if we increase the modulation, holding all other parameters fixed. We show results in Fig. 4 where $V/t = 200$ and find, as in Figs. 1 and 2, a single dominant peak. The physical origin of this peak is, however, quite different from before. It arises from a particular (depolarization-shifted) intersubband transition. By comparison with Fig. I 11 we see that the second such peak, which should be near $43t$, is missing while the third one is barely visible near $76t$. The reason for the absence of the second peak is the same as that for the absence of the second confined plasmon from Fig. 2: a parity selection rule valid because of inversion symmetry. More simply, the missing intersubband transition is dipole forbidden.

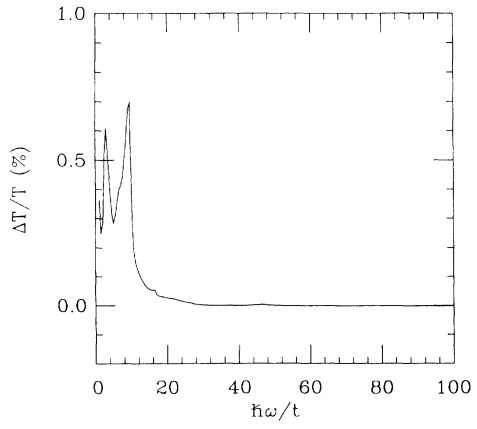

FIG. 3. Fractional change in transmission $\Delta T/T$ vs photon energy $\hbar\omega$. The modulation period has been decreased so the energy unit is now $t = 2.3$ meV. The LS2DEG and grating parameters are given in the text. No characteristic excitation dominates.

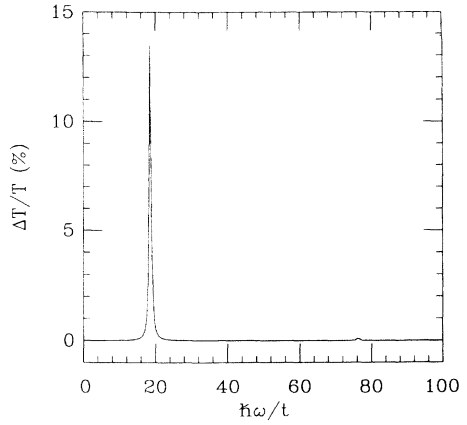

FIG. 4. Fractional change in transmission $\Delta T/T$ vs photon energy $\hbar\omega$. All parameter values are the same as for Fig. 3, except the KP barrier height which has been increased to $V/t = 200$. The dominant excitation is an intersubband transition.

As discussed in connection with Fig. 2, due to the strong modulation there is only a weak dependence of $\Delta T/T$ plots on grating parameters. Replacing $\rho_l \to \rho_h$ leaves the main peak location the same, but decreases its height to 4.4%. Going to the isolated LS2DEG limit shifts the main peak up by only $0.5t$ and changes its height to 4.0%. These small modifications remind us that the screening influence of the grating is less important for an intersubband transition than for a plasmon. Most of the former's energy is set by the single-particle transition energy, which is independent of the LS2DEG environment. The grating in our model only influences the depolarization shift.

In summary we note that for three of the four response regimes discussed in I we have found that the infrared-absorption spectrum is dominated by a sharp single peak. A necessary condition for this simple behavior is that $\mathrm{Im}\chi_{n,n}$ must show isolated peaks. The grating coupler then acts via parity constraints and factors of ρ_n^2 and $e^{-2G_n h}$ to reduce the number of these that appear in plots of $\Delta T/T$. When the spectrum of $\mathrm{Im}\chi_{n,n}$ is broadband, then so is that of $\Delta T/T$.

ACKNOWLEDGMENTS

This work was supported in part by the National Science Foundation through Grant Nos. DMR89-03851 and DMR91-13911. Some of the calculations were done on the Cray Research, Inc., Y-MP4/464 system at the National Center for Supercomputing Applications at the University of Illinois at Urbana-Champaign (Champaign, IL).

APPENDIX

We develop here the microscopic relations between currents and fields in the vicinity of the LS2DEG and grating coupler. The analysis is done assuming that the macroscopic wavelength of the infrared radiation, $1/\nu=2\pi c/\omega$, is much greater than any microscopic length, d, a, or h. The transverse fields may then be considered constants and the longitudinal fields treated in the electrostatic limit.[4] We write the total electric field near the surface as

$$\mathbf{E}=\mathbf{E}_T+\mathbf{E}_L\ , \tag{A1}$$

where $\mathbf{E}_T=e\hat{y}$ with fixed e is the transverse field and

$$\mathbf{E}_L(\mathbf{x})=\begin{cases}\displaystyle\sum_{n>0} r_n[\sin(G_n y),\cos(G_n y),0]e^{G_n x}, & x<0\\ \displaystyle\sum_{n>0}\{\lambda_n^{(-)}[-\sin(G_n y),\cos(G_n y),0]e^{-G_n x}+\lambda_n^{(+)}[\sin(G_n y),\cos(G_n y),0]e^{G_n(x-h)}\}, & 0<x<h\\ \displaystyle\sum_{n>0} t_n[-\sin(G_n y),\cos(G_n y),0]e^{-G_n(x-h)}, & h<x\ ,\end{cases} \tag{A2}$$

with $G_n=n(2\pi/d)$ is the longitudinal field. Our boundary conditions across $x=0$ and $x=h$ are that

$$\Delta\mathbf{E}_{\parallel}=0\ , \tag{A3}$$

$$\Delta\mathbf{D}_{\perp}=\frac{4\pi}{i\omega}(\nabla\cdot\mathbf{J})\ , \tag{A4}$$

where $\mathbf{D}$ is the displacement field given by multiplying $\mathbf{E}$ by the $\epsilon(x)$ of Eq. (1) and $\mathbf{J}$ is a two-dimensional current density. The Δ denote "the jump in value across an interface of." We distinguish between the current densities in the LS2DEG and the grating by using the superscripts s and g, respectively.

Requiring Eqs. (A3) and (A4) yields

$$r_n=\lambda_n^{(-)}+\lambda_n^{(+)}e^{-G_n h}\ , \tag{A5}$$

$$t_n=\lambda_n^{(-)}e^{-G_n h}+\lambda_n^{(+)}\ , \tag{A6}$$

$$\epsilon_s t_n-\epsilon_0[\lambda_n^{(-)}e^{-G_n h}-\lambda_n^{(+)}]=\frac{4\pi G_n}{i\omega}J_n^{(s)}\ , \tag{A7}$$

$$\epsilon_0[\lambda_n^{(-)}-\lambda_n^{(+)}e^{-G_n h}]+r_n=\frac{4\pi G_n}{i\omega}J_n^{(g)}\ , \tag{A8}$$

where the J_n's are cosine Fourier transforms of $J_y(y)$. The constitutive relations for these current densities are written as

$$J_n^{(s)}=\sigma(n,0)e+\sum_{m>0}\sigma(n,m)t_m,\quad n\geq 0 \tag{A9}$$

plus

$$r_n=\rho_0 J_n^{(g)}+\rho_n J_0^{(g)}+\tfrac{1}{2}\sum_{m>0}[\rho_{n+m}+\rho_{|n-m|}(1-\delta_{n,m})]J_m^{(g)},\quad n>0 \tag{A10}$$

and

$$e=\rho_0 J_0^{(g)}+\tfrac{1}{2}\sum_{m>0}\rho_m J_m^{(g)}\ , \tag{A11}$$

with the LS2DEG conductivity transform defined by Eq. (6) and the grating resistivity transform defined by Eq. (7). The asymmetric approach and appearance of Eq. (A9) versus Eqs. (A10) and (A11) arises from the physically different nature of conduction in the two planes. The $\sigma(n,m)$, as noted in Eqs. (8) and (9), are readily found from the χ^0 elements of I, while the typically large difference between ρ_h and ρ_l leads to convergence difficulties if one uses conductivities to describe the grating.[4]

There remains the algebraic task of reducing (A5)–(A11). We start by solving for the λ's from Eqs. (A6), (A7), and (A9) in terms of e and the t's. The results are combined with Eq. (A5) to produce equations for the t's (and hence the λ's) in terms of e and the r's. These are substituted into Eq. (A8) to yield

$$\sum_{m>0}F(n,m)r_m=\frac{4\pi}{c}J_n^{(g)}+\Gamma_n e\ , \tag{A12}$$

where

$$\Gamma_n=\sum_{l>0}\frac{\epsilon_0/n}{\sinh(G_n h)}D^{-1}(n,l)\frac{4\pi l}{c}\sigma(l,0)\ , \tag{A13}$$

$$F(n,m)=i\frac{\nu d}{n}\left\{[1+\epsilon_0\coth(G_n h)]\delta_{n,m}-\frac{\epsilon_0}{\sinh(G_n h)}D^{-1}(n,m)\frac{\epsilon_0}{\sinh(G_m h)}\right\}, \tag{A14}$$

and $D(n,m)$ is given by Eq. (10). We also can reexpress Eq. (5) as

$$\Sigma=\sigma(0,0)-\sum_{\substack{n>0\\ m>0}}\sigma(0,n)D^{-1}(n,m)\frac{4\pi i m}{c\nu d}\sigma(m,0)+\left[1+\sum_{\substack{n>0\\ m>0}}\sigma(0,n)D^{-1}(n,m)\times\frac{\epsilon_0}{\sinh(G_m h)}\left[\frac{r_m}{j_0}\right]\right]\left[\frac{j_0}{e}\right], \tag{A15}$$

where the unknowns are the fluctuating grating fields, i.e., the r's, and the averaged grating current $j_0 = J_0^{(g)}$. Independent equations for these come from the constitutive relations Eqs. (A10) and (A11). Define the dimensionless ratios for $n > 0$

$$j_n = J_n^{(g)} / J_0^{(g)} \ . \tag{A16}$$

Then Eqs. (A10) and (A11) yield

$$\frac{j_0}{e} = \left\{ \rho_0 + \tfrac{1}{2} \sum_{m>0} \rho_m j_m \right\}^{-1} , \tag{A17}$$

$$\frac{r_m}{j_0} = \rho_0 j_m + \rho_m + \tfrac{1}{2} \sum_{l>0} [\rho_{m+l} + \rho_{|m-l|}(1-\delta_{m,l})] j_l \ , \tag{A18}$$

so the quantities required in Eq. (A15) are determined by the fluctuating currents in the grating, the j_n's. The latter can be found by rewriting Eq. (A12) as

$$\sum_{m>0} F(n,m) \left[\frac{r_m}{j_0} \right] = \frac{4\pi}{c} j_n + \Gamma_n \left[\frac{e}{j_0} \right] \tag{A19}$$

and substituting from Eqs. (A17) and (A18).

For the limit of an isolated LS2DEG we make the following changes. Equations (3), (4), and (5) are replaced with

$$T = |t|^2 = 1 \Big/ \left| 1 + \frac{2\pi}{c} \Sigma \sqrt{\epsilon} \right|^2 , \tag{A20}$$

$$\Sigma = \sigma(0,0) + \sum_{n>0} \sigma(0,n) r_n / e \ , \tag{A21}$$

and the expansion of Eq. (A2) simplifies to

$$\mathbf{E}_L(\mathbf{x}) = \sum_{n>0} r_n \begin{cases} [\sin(G_n y), \cos(G_n y), 0] e^{G_n x}, & x < 0 \\ [-\sin(G_n y), \cos(G_n y), 0] e^{-G_n x}, & 0 < x \ . \end{cases} \tag{A22}$$

We only need further the matching condition Eq. (A4) and the constitutive relation Eq. (A9), with r_m replacing t_m.

*Present address: Basic Research Department, Electronics Technology Research Institute, Seoul, Korea.

[1] P. W. Park, A. H. MacDonald, and W. L. Schaich, preceding paper, Phys. Rev. B **46**, 12 635 (1992).

[2] D. Heitmann, in *Physics and Applications of Quantum Wells and Superlattices,* edited by K. v. Klitzing and E. E. Mendez (Plenum, New York, 1988), p. 317.

[3] J. Kotthaus, in *Interfaces, Quantum Wells and Superlattices,* edited by C. R. Leavens and Roger Taylor (Plenum, New York, 1988), p. 95.

[4] L. Zheng, W. L. Schaich, and A. H. MacDonald, Phys. Rev. B **41**, 8493 (1990).

[5] W. Hansen *et al.*, Phys. Rev. Lett. **58**, 2586 (1987).

[6] J. Alsmeier, Ch. Sikorski, and U. Merkt, Phys. Rev. B **37**, 4314 (1988).

[7] F. Brinkop, W. Hansen, J. P. Kotthaus, and K. Ploog, Phys. Rev. B **37**, 6547 (1988).

[8] T. Demel, D. Heitmann, P. Grambow, and K. Ploog, Phys. Rev. B **38**, 12 732 (1988).

[9] J. Alsmeier, E. Batke, and J. P. Kotthaus, Phys. Rev. B **40**, 12 574 (1989).

[10] *Electromagnetic Theory of Gratings,* edited by R. Petit (Springer, New York, 1980).

[11] L. Zheng and W. L. Schaich, Phys. Rev. B **43**, 4515 (1991).

[12] D. Liu and S. Das Sarma, Phys. Rev. B **44**, 9122 (1991).

[13] M. V. Krasheninnikov and A. V. Chaplik, Fiz. Tekh. Poluprovodn. **15**, 32 (1981) [Sov. Phys. Semicond. **15**, 19 (1981)].

[14] A. V. Chaplik, Surf. Sci. Rep. **5**, 289 (1985).

[15] U. Mackens, D. Heitmann, L. Prager, J. P. Kotthaus, and W. Beinvogl, Phys. Rev. Lett. **53**, 1485 (1984).